JCTC Journal of Chemical Theory and Computation

Article

pubs.acs.org/JCTC

Molecular Modeling of Triton X Micelles: Force Field Parameters, Self-Assembly, and Partition Equilibria

D. Yordanova, I. Smirnova, and S. Jakobtorweihen*

Hamburg University of Technology, Institute of Thermal Separation Processes, Eissendorfer Strasse 38, 21073 Hamburg, Germany

Supporting Information

ABSTRACT: Nonionic surfactants of the Triton X-series find various applications in extraction processes and as solubilizing agents for the purification of membrane proteins. However, so far no optimized parameters are available to perform molecular simulations with a biomolecular force field. Therefore, we have determined the first optimized set of CHARMM parameters for the Triton X-series, enabling all-atom molecular dynamics (MD) simulations. In order to validate the new parameters, micellar sizes (aggregation numbers) of Triton X-114 and Triton X-100 have been investigated as a function of temperature and surfactant concentration. These results are comparable with experimental results. Furthermore, we have introduced a new algorithm to obtain micelle structures from self-assembly MD simulations for the COSMOmic method. This model allows efficient partition behavior predictions once a representative micelle structure is available. The predicted partition coefficients for the systems Triton X-114/water and Triton X-100/water are in excellent agreement with experimental results. Therefore, this method can be applied as a screening tool to find optimal solute-surfactant combinations or suitable surfactant systems for a specific application.

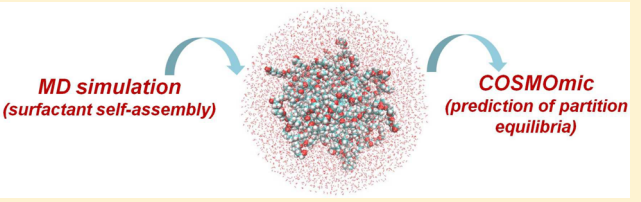

1. INTRODUCTION

Micelles are aggregates of amphiphilic molecules (surfactants). In aqueous solutions at concentrations higher than their critical micellization concentration (CMC) and temperatures above their critical micellization temperature surfactants form micelles. In these structures their hydrophilic part is directed toward the aqueous bulk phase, while their hydrophobic part is directed toward the center of the aggregates. With the help of micelles hydrophobic solutes can be solubilized in aqueous solution, since they can be incorporated in their hydrophobic core. The equilibrium of a solute between the micelle and the aqueous bulk phase can be quantified with a partition coefficient, which can be defined as a ratio of concentrations $P_i = c_i^{\text{micelle}}/c_i^{\text{water}}$. The partition coefficient is a decisive parameter regarding the selectivity and efficiency of micellar systems. These systems find application in food processing to solubilize different food ingredients,[1,2] as drug delivery agents in the pharmaceutical industry,[3,4] as separation media in chromatography and electrophoresis.[5] Furthermore, surfactant-based systems can be used in separation processes. Nonionic detergents are widely used as solubilizing agents in the isolation and purification of membrane proteins.[6−10] Several studies have shown that the Hydrophilic−Lipophilic Balance (HLB) values may be useful in selecting detergents for membrane protein extraction.[11,12] Detergents with HLB numbers between 12.4 and 13.5 (i.e., Triton X-114 and Triton X-100) were shown to be most efficient in solubilizing carboxypeptidase and mitochondrial proteins.[13,14] On the other hand, a low cloud point temperature (CPT) may be useful in membrane protein purification.[15−19] Increasing the temperature of a nonionic surfactant−water solution above the CPT leads to phase separation of the solution into a surfactant-rich phase and a solvent phase. This phenomenon is used in Cloud Point Extraction (CPE). For applications including proteins or living organisms it is important that the CPT is not much higher than a specific temperature. However, only a very limited number of nonionic surfactants have cloud points below 323 K. In this context, the nonionic surfactant Triton X-114 is of great interest for membrane protein extractions and also for technical surfactant based extraction processes.[20−27] Although the nonionic surfactants Triton X-114 and Triton X-100 were already used in various applications, their self-assembly was barely investigated. Since the self-assembly of surfactants to form micelles is a microscopic process (only a few molecules form one micelle), it is difficult to study via experiments. However, an alternative approach to study the process of micelle formation and to calculate thermodynamic properties of micellization is the application of molecular simulations. Therefore, the comparison of these Triton systems with theoretical methods is of great interest.

In this work all-atom molecular dynamics (MD) simulations were applied to study the self-assembly of Triton X-114 and Triton X-100 at different concentrations and temperatures. Due to its atomic scale, this approach gives very detailed information, but, on the other hand, it is computationally very demanding. To the best of our knowledge, this is the first time that the self-assembly of Triton X-114 and Triton X-100

Received: January 13, 2015

DOI: 10.1021/acs.jctc.5b00026
J. Chem. Theory Comput. XXXX, XXX, XXX−XXX

has been investigated with MD simulations. In the study of Buggert et al.,[28] MD simulations of a single Triton X-100 molecule in water and in *n*-octanol were performed in order to obtain Triton X-100 conformers for COSMO-RS calculations. The fundamental models behind every MD simulation are the interaction models (force fields). It is advantageous to use a force field that supports many different types of molecules, to open the possibility to study various mixtures (e.g., surfactant mixtures, protein−surfactant interactions, etc.).

The widely used CHARMM additive all-atom force field includes a wide range of chemical species, especially of amphiphilic molecules like lipids.[29,30] The CHARMM General Force Field (CGenFF) represents an extension of the CHARMM force field to drug-like molecules, which covers a wide range of chemical groups and makes it possible to perform simulations on drug-target interactions.[31] Moreover, a Web-based graphical user interface (*Micelle Builder* in CHARMM-GUI[32]) was developed to build pure and mixed micelles and protein/micelle complex systems. Since Triton X-molecules are not present in the CHARMM lipid force field nor in the CHARMM GenFF, the missing force field parameters were determined in this work.

As mentioned earlier partition coefficients are an important quantity in micelle applications, but it is computationally very demanding to determine them with MD simulations. One approach to predict partition equilibria, based on quantum chemistry and statistical thermodynamics, is the model COSMOmic.[33] COSMOmic is an extension of the "conductor-like screening model for realistic solvation" (COSMO-RS)[34−38] to anisotropic systems such as micellar systems and biomembranes. To predict partition equilibria with COSMOmic, the three-dimensional structure of a micelle is necessary. These structures can be taken from the MD self-assembly simulations. This approach (combination of MD and COSMOmic) has been already successfully applied for the prediction of micelle/water[39−41] and membrane/water[33,39,42−46] partition coefficients. Furthermore, it has been shown that free energy profiles for lipid bilayers from COSMOmic are in good agreement with profiles from MD simulations.[44,45] The combination of MD simulations and COSMOmic is advantageous due to the fact that a micelle once simulated with MD can afterward be used to predict partition behavior of various solutes, which makes the approach very computationally efficient.

In this work, the applicability of computer simulations for the prediction of partition behavior of neutral solutes in the systems Triton X-114/water and Triton X-100/water is demonstrated. Hence, the aims of this work are to determine the missing force field parameters for the Triton X-series and to study Triton X-114 and Triton X-100 self-assembly via MD simulations. Furthermore, micellar structures, obtained from self-assembly simulations, are used for partition equilibria predictions with the model COSMOmic.

2. METHODS

2.1. Parameter Optimization. The surfactant Triton X-114 is not directly included in the CHARMM36 force field nor in the CGenFF. The Force Field Toolkit (ffTK) (Version 1.0),[47] distributed as a VMD[48] plugin (VMD 1.9.2 alpha release), was used for the optimization of the missing parameters. The general parametrization procedure is fully described elsewhere,[31,47] and only a brief introduction is given here. The optimization is based on performing molecular mechanics (MM) calculations which should reproduce the quantum mechanics (QM) target data.[31] All QM calculations were performed using Gaussian03.[49] Initial guesses were obtained with the ParamChem tool.[50,51] ParamChem is an automated algorithm to assign force field parameters by analogy for the CGenFF. In addition, a "penalty score" is assigned to each parameter which judges the quality of the parameters. According to these penalties 8 atom charges, 1 bond, 4 angles, and 9 dihedrals were parametrized in this work, the penalties of these parameters were between 1 and 16. All other parameters were used from CGenFF version 2b7 as their penalties were zero. For further details about the ParamChem algorithm and the penalty score estimation, please refer to the corresponding publications.[50,51] CGenFF Lennard-Jones parameters were assigned to existing atom types. The molecular geometry was optimized at the MP2/6-31G(d) level of theory.

Charge optimization was based on compound-water interactions which were calculated with the scaled HF/6-31(d) model. The QM dipole moment was also used as target data. A complex between the molecule of interest in its MP2/6-31G(d) optimized geometry and a water molecule in the TIP3P[52] geometry was built for all hydrogen bond donors. The interaction distance was optimized at the HF/6-31(d) level of theory, keeping all other degrees of freedom fixed. The interaction energy was scaled by a factor 1.16, and the QM hydrogen bond length was offset by −0.2 Å to be relevant for the bulk phase.[31] The charge optimization was run iteratively in simulated annealing mode.[47]

The QM target data for the optimization of the bonded parameters was obtained from the Hessian computed at the MP2/6-31G(d) level of theory and scaled by 0.89.[31] The optimization was iteratively performed in downhill mode[47] weighting the geometry and energy terms 1:1.

A potential energy scan (PES) for each selected dihedral angle was calculated in 15° increments, starting from the optimized geometry. Two Gaussian input files were generated for each scan - one in the positive direction and one in the negative direction. Each structure was optimized at the MP2/6-31G(d) level of theory. The dihedral optimization was based on reproducing the QM PES. The first round of optimization was performed in simulated annealing mode. Several refinement optimizations were run, again in simulated annealing mode. A final refinement was performed in downhill mode.[47]

The obtained parameters are applicable for all surfactants of the Triton X-series as they differ only in the length of the polyoxyethylene chain. In this work we validated the parameters with simulations of Triton X-114 and Triton X-100.

2.2. Molecular Dynamics Simulations. The MD simulations were performed using the GROMACS package version 4.6.5.[53] The CHARMM36 force field was chosen due to its good parametrization of amphiphilic molecules like lipids and surfactants.[29,30,54] Triton X-114 was modeled with CGenFF,[31] whereas the missing parameters were determined in this work. The parameter optimization was discussed in detail in the previous section. Water was modeled with CHARMM TIP3P.[55,56]

For a pure Triton X-114 simulation, a rectangle box containing 450 Triton X-114 molecules was constructed by placing a copy of the molecule on each grid point of a rectangle 2.625 × 10.5 × 15 lattice. After an energy minimization with the steepest descent method, a short simulation in the NPT ensemble was conducted for 400 ps, using the Nosé−Hoover thermostat with the coupling time constant of 1 ps at T =

DOI: 10.1021/acs.jctc.5b00026
J. Chem. Theory Comput. XXXX, XXX, XXX−XXX

Table 1. System Configurations for MD Simulations of Triton X-114 and Triton X-100 in Aqueous Solution

	no. of molecules					
surfactant	surfactant	water	total no. of atoms	$C_{surfactant}$ [mol/L]	temp [K]	simulation time [ns]
TX114	216	53352	180144	0.22	283	100
TX114	216	53371	180201	0.22	283	100
TX114	216	53360	180168	0.22	313	100
TX114	216	53360	180168	0.22	283	200
TX114	216	120515	381633	0.1	283	200
TX100	216	53407	183333	0.22	283	200

298.15 K and the Berendsen barostat (isotropic, coupling constant τ_p = 5 ps). As the volume was far from equilibrium and for a rapid equilibration, the pressure was set to 500 bar in this short equilibration step. Afterward, the equilibrated box has been simulated in the NPT ensemble for 12 ns, using the Nosé−Hoover thermostat at T = 298.15 K and the Parrinello−Rahman barostat at p = 1 bar.

To obtain initial configuration for the MD simulations, a specific amount of Triton X-114 monomers was placed randomly into a cubic water box, whereby overlapping water molecules were removed, to match a specific concentration. The energies of the initial configurations were minimized with the steepest descent method. After the energy minimization, a simulation in the NVT ensemble was conducted for 600 ps to further relax the system, using the Nosé−Hoover thermostat with the coupling time constant of 1 ps and T = 298 K. After these initialization steps, all simulations were performed in the NPT ensemble at p = 1 bar and T = 283 K or T = 313 using the Nosé−Hoover thermostat (coupling constant τ_t = 1 ps) and the Parrinello−Rahman barostat (coupling constant τ_p = 2 ps). For the NPT simulations a time step of 0.002 ps has been used. The Lennard-Jones interactions were cut off at 1.2 nm and switched from 0.8 nm on, where both the potential and the force were switched. For the Coulomb interactions, a real space cutoff of 1.0 nm was applied. For long-ranged electrostatic interactions the Particle Mesh Ewald method[57,58] was used. All bonds to hydrogens were constrained with the LINCS algorithm.[59]

To reach a specific concentration, a defined amount of surfactant monomers has to be placed into a cubic water box. The self-assembly of Triton X-114 was studied at two different concentrations: C_{TX114} = 0.22 mol/L and C_{TX114} = 0.1 mol/L. Additionally, a simulation of Triton X-100 self-assembly at C_{TX100} = 0.22 mol/L was performed. A summary of all MD simulations is given in Table 1.

2.3. Analysis Methods. In order to identify distinct micelles, a method to define the micelles boundaries is necessary. One efficient approach, developed and validated by Sammalkorpi et al.,[60] is the definition via distances between the center of mass of surfactant monomers and selected carbon atoms. This technique was adapted for the nonionic surfactants Triton X-114 and Triton X-100. Small micelles tend to be in close vicinity before they aggregate into larger aggregates due to the fact that nonionic surfactants have a larger headgroup compared to its tail group. To take this effect into account, distances between three carbon atoms of all surfactants are considered but not the center of mass of the monomers. This procedure was already used for the nonionic surfactant Brij35 in our previous publication.[41] In the case of Triton X-114, the distances between the C1D, C1A, and C5 atoms (see Figure 2) of all surfactants have been calculated. Any two Triton X-114 molecules are defined to be part of the same micelle if (1) one of these three distances is shorter than $R1_{cut}$ = 0.58 nm, or (2) two out of three distances are shorter than $R2_{cut}$ = 0.78 nm, or (3) all three distances are shorter than $R3_{cut}$ = 1.00 nm. These cutoffs were chosen after detailed visualization of the configurations to verify a good definition of micelles. The same carbon atoms and cutoffs were used for the definition of Triton X-100 micelles.

The shape of micelles has been analyzed by examining the eccentricity ε,[61,62] which is defined as

$$\varepsilon = 1 - \frac{I_{min}}{I_{avg}} \quad (1)$$

where I_{min} is the moment of inertia along the principal axes with the smallest magnitude, whereas I_{avg} is the average of all three moments of inertia. ε can have values from 0 to 1, inclusive. For simple, closed aggregates, ε = 0 usually corresponds to a highly symmetrical shape resembling a sphere, while larger values of ε correspond to progressively more elliptical shapes.[61,62]

The radius of gyration of the micelles is calculated as the root-mean-square distance between the center of mass of the micelle and its ends. If the micelle is a sphere, the radius of this sphere R_s can be calculated from the relation to the radius of gyration

$$R_s = \sqrt{\frac{5}{3}} R_g \quad (2)$$

2.4. The Model COSMOmic. The model COSMOmic,[33] an extension of COSMO-RS[34−38,63] for anisotropic systems such as micelles and bilayers, was applied for the prediction of partition behavior of various solutes in the micellar systems. The COSMOtherm (version C3.0 Release 13.01) implementation of COSMO-RS and COSMOmic with the BP_TZVP_C30_1301 parametrization is used throughout this work. The model is based on statistical thermodynamics and quantum chemical calculations and takes the three-dimensional structure of a micelle into account. The concept of COSMOmic is to divide the micelles radially into several layers. For each layer COSMO-RS calculations of the solute in different orientations are performed; whereas the composition within a layer is assumed to be homogeneous, and each layer has a specific atomic composition of surfactant atoms and water. To predict partition equilibria with COSMOmic, the atomic distribution in the micelle/water system and the structure of a surfactant monomer have to be known. Surfactant monomer and micelle structures from MD simulations are used. It is of major importance to obtain the surfactant conformer from the correct environment, as molecules can have different configurations in different media.[28,43,64] Thus, the surfactant conformers were taken out of the self-assembly simulations. The selection of a representative surfactant monomer was done with respect to the solvent accessible surface. In our previous work,[43] we demonstrated the usage of a

DOI: 10.1021/acs.jctc.5b00026
J. Chem. Theory Comput. XXXX, XXX, XXX−XXX

lipid conformer, which has a solvent accessible surface close to the average solvent accessible surface within the considered lipid bilayer. It was shown that the micelle structures have also an influence on the prediction quality of COSMOmic.[40,41] However, a detailed analysis has not been performed. Furthermore, for the combination of MD and COSMOmic it was recommended to use average atomic distributions for the COSMOmic calculations.[43] Although single micelle structures can give good results, using averaged atomic distributions is more reliable and physically reasonable.[40,43]

COSMOmic also requires DFT/COSMO files for all components of the system and all solutes of interest. These DFT/COSMO files were calculated with Turbomole 5.10[65] on the BP-TZVP[66−68] level and the RI (resolution of the identity) approximation.[69] A conformer analysis of the solute molecules has been performed with HyperChem 8.0.[70]

For further details about the models COSMOmic and COSMO-RS, please refer to the corresponding publications.[33−38,40,43,63]

3. RESULTS AND DISCUSSION

3.1. Parameter Optimization Overview. We have obtained CGenFF parameters for Triton X-114 molecule using the ffTK.[47] In line with the CHARMM force field philosophy,[31] two smaller molecules representing the hydrophobic part of Triton X-114 were used for the parameter calculations. The parameters were first optimized for the smaller molecule in order to get better initial guesses for subsequent iterations. Schematic illustration of the Triton X-114 structure and the two smaller molecules are presented in Figure 1. Note that when a covalent link is formed to create a

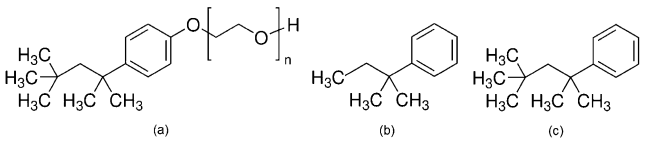

Figure 1. (a) Structural formula of Triton X-114 (n = 7−8) and Triton X-100 (n = 9−10); in the performed MD simulations Triton X-114 and Triton X-100 were modeled with n = 8 and n = 10, respectively. (b) Structural formula of model compound (1): 1,1-dimethylpropylbenzene; (c) structural formula of model compound (2): 1,1,3,3-tetramethylbenzene.

larger molecule from model compounds, the charge on the deleted H is added to the adjacent oxygen to maintain an integer charge. The parametrization was carried out in a self-consistent fashion by applying the following sequence:

1. Optimization in four steps, where first charges, second bonds, then angles, and in the end dihedrals of model compound (1) (see Figure 1b), are obtained.
2. Second iteration of Step 1.
3. Reoptimization of C2, C4, and C5 charges, bonds, angles, and dihedrals in model compound (2), for atom names and molecule structures see Figures 1c and 2.
4. Second iteration of Step 3 until reaching convergence to reproducible values.

The atoms, whose partial charges were optimized, are shown in Figure 2. According to the CHARMM force field,[31] the charges of the nonpolar hydrogens were assigned a fixed charge of +0.09. Aromatic C−H groups were assigned the standard CHARMM charges of −0.115 and +0.115 on carbon and hydrogen atoms, respectively. The charges of the three carbon

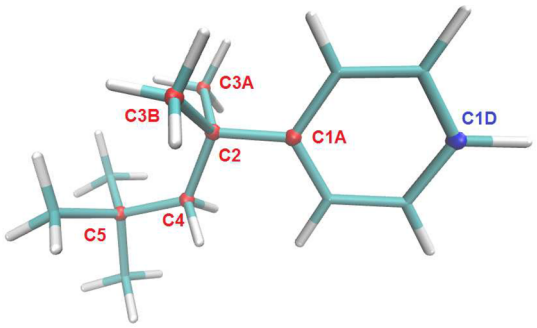

Figure 2. 3D structure of 1,1,3,3-tetramethylbenzene (model compound (2)); the atoms for which the atomic charges were optimized are shown in red, and the other carbon atoms used in the analysis are shown in blue.

atoms that are not optimized are taken from the CGenFF (they show a penalty of zero in the ParamChem tool). QM calculations for interactions between the model compounds and water molecules have been computed following the standard CGenFF procedure. The interaction properties of the final optimization are listed in Table 2. The optimized partial charges are given in Table S1 of the Supporting Information.

Ideally, the compound-water energies should be within 0.2 kcal/mol from the QM interaction energies.[31] Some of the final MM energies differ by more than 0.2 kcal/mol from the target

Table 2. Optimized 1,1,3,3-Tetramethylbenzene (Model Compound (2))-Water Interaction Energies and Geometries

	interaction energy (kcal/mol)	interaction distance (Å)
interaction geometry	$\Delta E(QM-MM)$	$\Delta r(QM-MM)$
H1A···OHH	−0.385	−0.050
H1B···OHH	0.503	0.250
H1C···OHH	0.585	0.300
H1D···OHH	0.617	0.300
H1E···OHH	0.545	0.300
H3A···OHH	0.401	0.150
H3B···OHH	0.128	0.300
H3C···OHH	0.165	0.150
H3D···OHH	0.165	0.150
H3E···OHH	0.401	0.150
H3F···OHH	0.128	0.300
H4A···OHH	−0.052	0.150
H4B···OHH	−0.052	0.150
H6A···OHH	0.094	0.100
H6B···OHH	0.094	0.100
H6C···OHH	0.527	0.200
H6D···OHH	0.196	0.150
H6E···OHH	0.238	0.250
H6F···OHH	0.523	0.200
H6G···OHH	0.238	0.250
H6H···OHH	0.196	0.150
H6I···OHH	0.476	0.200
AD[a]	0.249	0.182
AAD[a]	0.317	0.204
RMSD[a]	0.358	0.209

[a]AD, average deviation; AAD, average absolute deviation; RMSD, root-mean-square deviation.

DOI: 10.1021/acs.jctc.5b00026
J. Chem. Theory Comput. XXXX, XXX, XXX−XXX

data, but the agreement is satisfactory considering that the matching of all 22 interaction energies is complicated for a large molecule like model compound (2). Deviations in this range are also reported for optimized CGenFF parameters for phosphonosulfonimidate.[71] The interaction distances are overestimated by 0.1−0.3 Å (see Table 2). As shown in Table 3, the dipole moment is overestimated by 47% compared to the MP2 value, which is in the desirable range to reproduce bulk phase properties.[31]

Table 3. Gas Phase Dipole Moment of Model Compound (2) Calculated at the MP2/6-31G(d) and MM Level of Theory

μ	QM	MM
X	−0.305	−0.381
Y	−0.055	−0.249
Z	0.000	0.000
total	0.310	0.456

Table 4 represents the optimized bonded parameters along with the QM results. QM bond length is reproduced within 0.3 Å, as desirable.[31] MM optimized angles are all within 3°, except for C2−C4−C5 angle which shows a deviation of 10°. However, the result is considered as reasonable, because it is in the range of the CGenFF value (113.50°), for which the ParamChem tool shows a penalty as low as 1.8. The optimized bonds and angles parameters are given in Table S2 in the Supporting Information.

Table 4. QM and MM Optimized Equilibrium Geometry of Model Compound (2)

coordinate	QM	MM	difference
Bond Lengths (Å)			
C1A−C2	1.5426	1.5420	−0.0006
Angles (°)			
C1B−C1A−C2	121.58	121.80	0.22
C1A−C2−C4	108.80	108.40	−0.4
C1A−C2−C3A	107.56	108.70	1.14
C2−C4−C5	126.24	116.24	−10.0

Figure 4 shows a comparison between the target QM, initial MM, and refined MM PESs of 8 optimized torsion angles (see also Figure 3). All optimized dihedral angles are given in Table S3 of the Supporting Information. The refined MM parameters are in excellent agreement with the QM PESs. The RMSE between the QM and the refined MM PESs for all 8 dihedral angles is 0.125. One dihedral from the hydrophilic poly(ethylene oxide) chain (hydrophilic head) of Triton X-114 was separately optimized, and ethylene glycol monomethyl ether was used for this optimization (see Figure 5). The refined MM parameters yield a PES that reproduces the QM target PES with excellent agreement (RMSE = 0.044). A comparison between the MP2/6-31G(d), initial MM, and refined MM PESs is shown in Figure 6.

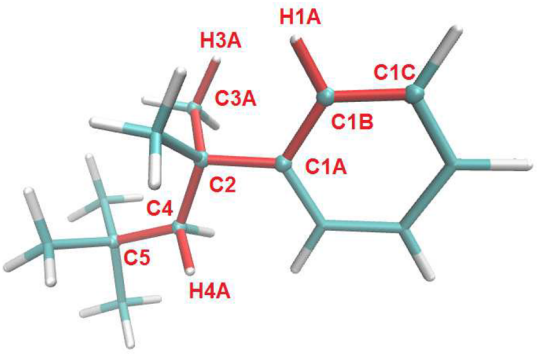

Figure 3. 3D structure of 1,1,3,3-tetramethylbenzene (model compound (2)); the atoms comprising the 8 dihedral angles which were optimized in this molecule are shown in red.

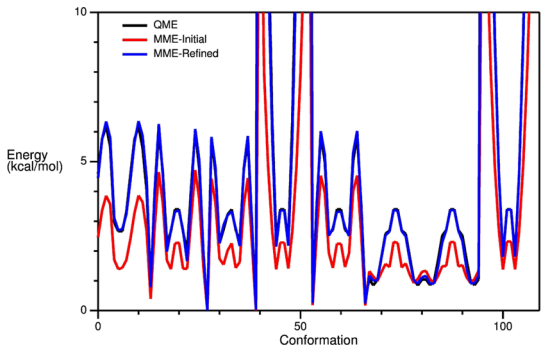

Figure 4. Potential energy scans for the 8 optimized dihedral angles of model compound (2), shown in one plot. The abscissa depicts the number of the scan point. The ordinate is the relative energy in kcal/mol: QM PES (black); using the initial guess parameters (red); using the optimized parameters (blue). The results were visualized with ffTK.[47]

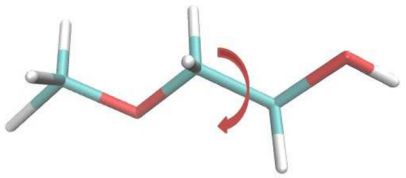

Figure 5. Structure of ethylene glycol monomethyl ether used for optimization of one dihedral from the hydrophilic head region of Triton X-114.

To validate the determined force field parameters usually some physical and thermodynamic quantities (density, enthalpy of vaporization, energy of solvation) are calculated and compared with experimental measurements.[31,47] The density

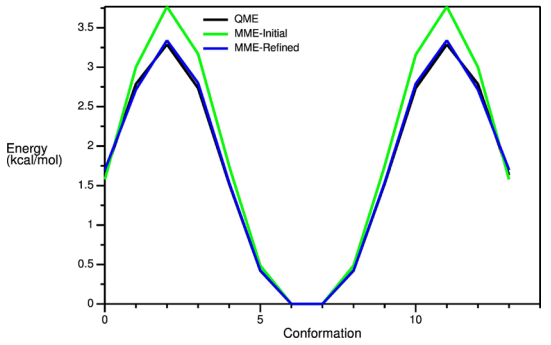

Figure 6. Potential energy scans of one optimized dihedral from the hydrophilic poly(ethylene oxide) chain. The abscissa depicts the number of the scan point. The ordinate is the relative energy in kcal/mol: QM PES (black); using the initial guess parameters (green); using the optimized parameters (blue).

DOI: 10.1021/acs.jctc.5b00026
J. Chem. Theory Comput. XXXX, XXX, XXX−XXX

of Triton X-114 was determined from a MD simulation at 298 K. This (1.055 g/cm^3) is in excellent agreement with the experimental value of 1.052 g/cm^3.[23] To the best of our knowledge, experimental data for other pure Triton X-114 properties, which can be used for parameter validation, are not available.

3.2. Self-Assembly of Triton X-114 and Triton X-100 in Aqueous Solution. MD simulations of Triton X-114 and Triton X-100 in aqueous solution have been performed. The simulations started from a random configuration of surfactants to study the self-assembly at different concentrations. The simulated concentrations (C = 0.22 mol/L and C = 0.1 mol/L) are both orders of magnitude above the CMC of Triton X-114 (0.17 mM[72]). Unfortunately, lower concentrations were not considered due to limitations of the system size. The simulated systems are already very large (see Table 1), consequently computationally very demanding. However, according to the phase diagram of the Triton X-114/water system, it is in the liquid phase at this concentration.[73] The system Triton X-100/water is also in the one phase region at the considered concentration.[74]

In Figure 7 the progress of the maximum aggregation number over the simulation time at two different concentrations of Triton X-114 is shown. The aggregation numbers of the observed micelles vary between 30 and 216 over the MD trajectories. It is actually known that nonionic surfactants have a wider distribution of micelle sizes than ionic surfactants.[75−77]

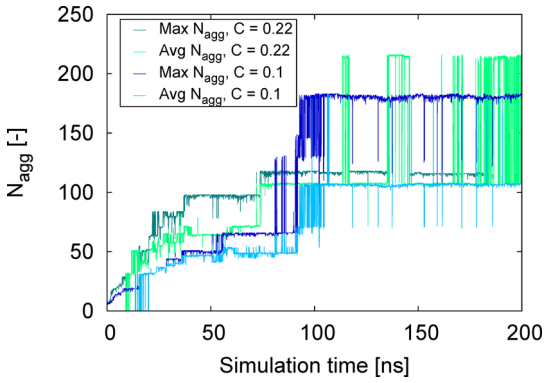

Figure 7. Maximum and average aggregation number of Triton X-114 at different concentrations: C_{TX114} = 0.22 mol/L (blue) and C_{TX114} = 0.1 mol/L (cyan); T = 283 K.

In the system with a concentration of C_{TX114} = 0.22 mol/L, small aggregates consisting of 30−40 surfactant molecules were formed after 10 ns. In the first 100 ns of the simulation micelles in close proximity were observed (see Figure 8). The assembly of small aggregates into larger micelles (∼100 surfactant monomers) starts at 40 ns. The maximum aggregation number after 100 ns is around 120. Due to the slow self-assembly, longer simulation times of 200 ns have been performed. At 120 ns, all surfactants begin to aggregate into one micelle (216 surfactant monomers). At the lower concentration (C_{TX114} = 0.1 mol/L) small micelles with aggregation numbers around 30 were observed after 25 ns. The maximum aggregation number after 50 ns is around 60, and after 100 ns smaller aggregates start to aggregate to a larger micelle with an aggregation number of 183. The maximum aggregation number over the 200 ns MD trajectory is 183 (lower than 216 at the higher concentration of C_{TX114} = 0.22 mol/L). Due to the fact, that at the lower concentration two times more water is present, the micellization process is slower. Smaller aggregates were observed compared to results at the higher concentration. It is obvious from the simulation data, shown in Figure 7, that the micelle formation is faster at higher concentrations, which corresponds to other literature data.[40,60] As there are still fluctuations of the aggregation number at the higher concentration, the equilibrium condition in this system may not have been reached. Since at the lower concentration the aggregation process is slower, one can assume that longer simulation times are needed for this system to reach complete equilibration. Therefore, we expect that with enough simulation time both systems would converge to a single large micelle containing all 216 monomers. However, this simulation time is considered as sufficient for the purpose of this work.

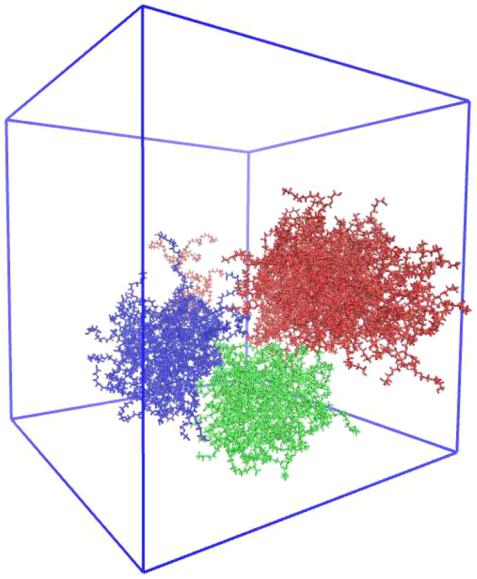

Figure 8. A snapshot of Triton X-114 self-assembly simulation at C_{TX114} = 0.22 mol/L after 100 ns. With different colors are shown 3 different micelles (aggregation numbers 120, 48, 48). For a clear presentation of the micelles, water and the monomers were removed in this snapshot.

The probabilities of the aggregation numbers can be calculated from the MD simulations. The aggregation number probabilities for Triton X-114 at C_{TX114} = 0.22 mol/L and at C_{TX114} = 0.1 mol/L are shown in Figure 9. Note that these distributions characterize the self-assembly process and not an equilibrated system. Aggregates consisting of less than 30 monomers are not considered as micelles, as the smallest stable micelles have an aggregation number of ca. 30. Figure 9 illustrates the results of five independent simulations, which were started from different starting configurations for different concentrations and temperatures. The probabilities were calculated for t > 40 ns, when the first stable micelles were observed (see Figure 7). It is evident, that the aggregation numbers are not the same for all simulations but are in the same range. Due to the shorter simulation time (100 ns) of the two independent simulation runs at C = 0.22 mol/L, the most probable micelle sizes (30−40) are smaller than the most probable aggregation numbers from the system simulated for 200 ns (95−120) (see Figure 9). Wolszczak and Miller[78] reported experimentally determined aggregation numbers of N_{agg} = 68 and N_{agg} = 156, dependent on the used fluorometric techniques. The measurements were carried out at T = 22 °C

DOI: 10.1021/acs.jctc.5b00026
J. Chem. Theory Comput. XXXX, XXX, XXX−XXX

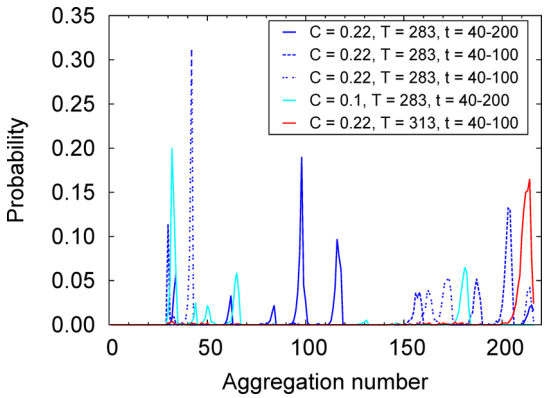

Figure 9. Probabilities of the aggregation numbers for Triton X-114 at different concentrations and temperatures. The concentrations C are given in mol/L, the temperatures T have units of K, and the simulation times t are given in ns.

and detergent concentration of C = 0.01 mol/L. Aggregation numbers determined at surfactant concentration much greater than the critical micelle concentration may differ strongly from the aggregation numbers around the CMC.[72] The experimental results of Wolszczak and Miller and our simulations are both orders of magnitude above the CMC (0.17 mM[72]); therefore, a quantitative comparison is still not possible. However, the simulated values are in the range of the experimental aggregation numbers.

In order to investigate the influence of temperature on the aggregation process, an additional 100 ns simulation of 0.22 mol/L Triton X-114 solution with 216 surfactant molecules has been performed at a temperature above the CPT. The other simulations were all performed at T = 283 K, whereas the CPT of Triton X-114 at this surfactant concentration is 300 K.[79] In Figure 10, the growth of the micelles in terms of the largest

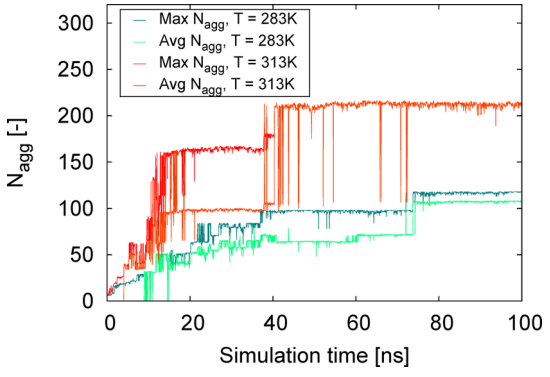

Figure 10. Maximum and average micelle size over time from two self-assembly simulations of the same Triton X-114/water system at 283 K (blue) and at 313 K (red).

aggregation number are presented. Corresponding to experimental results, at temperatures above the CPT the micellization process is faster and the micelle size increases.[80] Our simulations are in agreement with these findings, as self-assembly is faster and the largest micelles are more stable. However, as shown in Figure 7 also at the lower temperature the micelle size will increase further for longer simulation times.

As the determined force field parameters can be used for all molecules of the Triton X-series and as Triton X-100 is also widely used, a single 200 ns simulation of Triton X-100 self-assembly has been performed. As already observed in the Triton X-114 self-assembly simulations, during the first 50 ns of the simulation small aggregates consisting of 30−40 surfactant monomers were formed. Larger micelles with aggregation number around 190 were observed after 60 ns, and after 130 ns almost all Triton X-100 monomers aggregate to one micelle with an aggregation number of N_{agg} = 214. Patel et al.[81] reported an experimentally determined Triton X-100 aggregation number of N_{agg} = 287. Since the experimental aggregation number is larger than the total number of surfactant molecules in the simulation, it is expected that all monomers converge to one micelle. An increase of the system size would probably show even larger micelles.

3.3. Prediction of Partition Equilibria with COSMOmic.

To predict the micelle/water partition behavior of solute molecules with COSMOmic, a micelle structure is required. Since the model COSMOmic needs the spatial composition of the system, the use of proper micelle structures is crucial for the predictive quality. In the study of Storm et al.[40] single micelle structures were used as input for the COSMOmic calculations, whereas thousands of single micelles have been selected in order to achieve statistical reliable results. A more physically reasonable approach is to use averaged atomic distributions as input structures for the COSMOmic calculation.[43] In this work, averaged atomic distributions of the most probable micelle structures, which have been obtained during the MD simulations, have been calculated and selected. This procedure was previously suggested for bilayers, and it was demonstrated that using averaged atomic distributions from MD simulations as input for the model COSMOmic is beneficial.[43] In order to achieve statistically reliable results, the atomic distribution were averaged over at least 200 micelles in this work. Note that especially the small micelle sizes used as input for the COSMOmic calculations are not stable in the simulations. These aggregation numbers are not considered as comparable with experimental results. However, the aim is to study the influence of the micelle structure (size and shape) in the prediction with the model COSMOmic.

In the study of Storm et al.[41] the influence of the water shell structure on the prediction quality was analyzed. Gaps in the water layer around some micelles were observed, resulting from another micelle in close proximity. When using these structures as input for COSMOmic, a decline in the prediction quality was observed. In order to overcome the effect of outliers, resulting from a deficient water layer around the micelle, an approach to fill up the gaps in the water shell was applied in this work. If atom i of a surfactant molecule, which is not part of the micelle, was present in the atomic distribution, it was subsequently replaced by an equivalent amount of water molecules. This amount was calculated by

$$N_{SOL,fill} = \frac{n_{SOL}}{n_{SURF}} \frac{m_{SURF,i}}{M_{SURF}} \quad (3)$$

where n is the molecular bulk density (here are the input parameters), M is the molecular weight, and m is the mass of an atom. The subscripts denote the surfactant and solvent molecule. It is important to note that only the values of the water molecules were altered by this method, no atoms were placed into space. In order to validate this approach, the radial density of water around a micelle was analyzed (Triton X-114 micelle with N_{agg} = 33). The micelle structure was obtained from a self-assembly simulation (see Table 5). The same micelle was also separately simulated in a system containing

DOI: 10.1021/acs.jctc.5b00026
J. Chem. Theory Comput. XXXX, XXX, XXX−XXX

Table 5. Structure Parameters of Averaged Triton X-114 Micelles, the Angular Brackets Donate That These Values Were Averaged over the Micelles

N_{agg}	no. of micelles	$\langle\varepsilon\rangle$	$\langle R_g\rangle$ [nm]	$\langle R_s\rangle$ [nm]
32[a]	1673	0.17 ± 0.07	1.72 ± 0.04	2.22 ± 0.05
33[b]	440	0.18 ± 0.06	1.77 ± 0.04	2.28 ± 0.05
65[a]	465	0.33 ± 0.06	2.26 ± 0.06	2.92 ± 0.08
98[b]	1265	0.42 ± 0.03	2.62 ± 0.05	3.38 ± 0.06
116[b]	633	0.64 ± 0.03	3.15 ± 0.10	4.06 ± 0.13
181[a]	511	0.30 ± 0.03	3.26 ± 0.07	4.21 ± 0.09

[a]The micelle structures used for COSMOmic calculations were taken from a 200 ns MD simulation of 0.1 mol/L Triton X-114 solution. [b]The micelle structures used for COSMOmic calculations were taken from a 200 ns MD simulation of 0.22 mol/L Triton X-114 solution.

otherwise only water. Therefore, a snapshot of the self-assembly simulation, containing a N_{agg} = 33 micelle, was taken, and all other Triton X-114 molecules were removed. After a short equilibration simulation, the system was simulated for 40 ns. In this case, no gaps in the water layer can occur, as there is only one micelle in the system. Therefore, the radial distribution of water from this system corresponds to a complete water layer. As COSMOmic assumes the second phase for the partition coefficient calculations to be the last layer, the densities far away from the micelle should represent bulk water for micelle/water partition coefficient predictions. Hence, the densities around the different micelles should level off at the same water density. However, by comparing the densities for the micelle from the self-assembly simulation with the density of the micelle surrounded by water only, it can be seen that they converge to different values (see Figure 11). This is due to

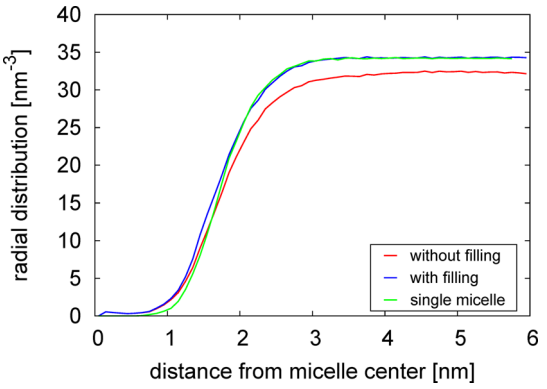

Figure 11. Radial density of the oxygen atom of water around a micelle with 33 Triton X-114 molecules: calculated from a self-assembly simulation without filling up the gaps in the water shell (red); calculated from the same self-assembly simulation, whereas the gaps in the water shell were filled up (blue); calculated from a simulation of a single micelle in a water box (green).

other micelles and surfactant molecules in the self-assembly simulation. However, when the gaps are filled with the described approach, the radial density overlap with the density from the simulation of a single micelle (see Figure 11). Therefore, it can be concluded,that the applied approach successfully generates structures with complete water shells around the micelle. In this study all atomic distributions are calculated with this approach.

The selected micelle sizes (aggregation number), their sampling (number of averaged micelles per atomic distribution), eccentricity ε, radius of gyration R_g, and radius of the micelle R_s are presented in Table 5. These micelle structures were used for the prediction of the partition behavior of 10 solutes within COSMOmic. We selected solutes for which experimental partition coefficients are available. Furthermore, here we only considered experimental data in which the pH-value was chosen such that the solute was in its neutral state. The predicted partition coefficients (log$P$) between Triton X-114 micelle and water in comparison with experimental data are given in Table 6. The RMSE (root-mean-square error) is defined as

$$\mathrm{RMSE} = \sqrt{\frac{1}{n}\sum_{i=1}^{n}\left(\log P^{\mathrm{MW,COSMOmic}} - \log P^{\mathrm{MW,exp}}\right)^2} \quad (4)$$

where n is the number of solutes for which COSMOmic calculations were carried out. All experimental data of the partition coefficients in the system Triton X-114/water is taken from the study of Ingram et al.[79] with a maximum experimental error of ±0.1.

To study the influence of the micelle size and shape on the COSMOmic results, different micelles were used for the COSMOmic calculations. By comparing the RMSE of all logP^{MW} values presented in Table 6, no significant differences for the range N_{agg} = 32−98 can be observed, since all overall RMSEs are similar (∼0.40). The predicted partition coefficients slightly overestimate the experimental values but still provide good prediction quality. The calculated partition coefficients using micelles with aggregation numbers in the range of the experimental values (N_{agg} = 116−181) are in very good agreement with experimental results, since the RMSE = 0.27. This RMSE is lower than the obtained in the original COSMOmic article for bilayers.[33] When using larger micelles ($N_{agg} \geq 100$) as input for the COSMOmic calculations, the tendency to overestimate the partition coefficients is reduced. However, usually it is expected that larger micelles are less suitable for COSMOmic as it is more likely that their shape deviates from a sphere.[41] Nevertheless, here larger micelles show a slight increase in prediction quality, which is probably due to the set of solutes used here. More diverse experimental data is necessary for a final judgment. A reason could be a different arrangement of surfactants within the micelle. Although the eccentricity for N_{agg} = 181 is only 0.3, the structure is not a sphere where the end atoms of the heads are all located on the surface. By visual inspection of only the hydrophobic region of a micelle of this size it seems that this region has a shape similar to a dumbbell, probably because two micelles are aggregated to one large micelle. Furthermore, the radial densities show water close to the hydrophobic core. The eccentricity shows still a small value as all atoms are forming a sphere and only by visual inspections and by the radial densities it becomes obvious that this is not a perfect micelle structure. Hence, especially the radial density should also be checked before a micelle is used for COSMOmic.

The structural parameters (eccentricity factor ε, radius of gyration R_g, and radius of the micelle R_s) of averaged Triton X-100 micelles are given in Table 7. Predicted partition coefficients of 6 neutral solutes between Triton X-100 micelles and water in comparison with experimental results[82,83] are shown in Table 8.

The calculated partition coefficients using small Triton X-100 micelle structures (N_{agg} = 33 and N_{agg} = 34) are in excellent

DOI: 10.1021/acs.jctc.5b00026
J. Chem. Theory Comput. XXXX, XXX, XXX−XXX

Table 6. Predicted Partition Coefficients of 10 Neutral Solutes in Triton X-114 Micelles in Comparison with Experimental Data[79]

	$\log P^{MW,COSMOmic}$						
solute	N_{agg} = 32[a]	N_{agg} = 33[b]	N_{agg} = 65[a]	N_{agg} = 98[b]	N_{agg} = 116[b]	N_{agg} = 181[a]	$\log P^{MW,exp}$
diclofenac	4.01	4.02	4.01	4.07	3.86	3.47	3.82
ibuprofen	4.26	4.23	4.09	4.10	3.93	3.40	3.73
salicylic acid	2.95	2.97	2.95	2.98	2.78	2.64	2.23
ferulic acid	2.71	2.78	2.76	2.77	2.57	2.53	2.20
phenol	2.00	2.01	2.00	2.02	1.84	1.79	1.65
syringic acid	1.78	1.81	1.85	1.85	1.67	1.78	1.64
coumaric acid	2.04	2.12	2.22	2.26	2.06	2.17	2.19
vanillic acid	1.87	1.92	2.03	2.06	1.87	1.99	1.88
vanillin	2.05	2.11	2.08	2.07	1.89	1.89	1.49
hydroxybenzoic acid	1.92	1.96	2.05	2.09	1.90	2.00	1.83
RMSE	0.40	0.42	0.40	0.41	0.27	0.27	

[a]The micelle structures used for COSMOmic calculations were taken from a 200 ns MD simulation of 0.1 Triton X-114 solution. [b]The micelle structures used for COSMOmic calculations were taken from a 200 ns MD simulation of 0.22 Triton X-114 solution.

Table 7. Structure Parameters of Averaged Triton X-100 Micelles, the Angular Brackets Donate That These Values Were Averaged over the Micelles

N_{agg}	no. of micelles	$\langle\varepsilon\rangle$	$\langle R_g\rangle$ [nm]	$\langle R_s\rangle$ [nm]
33[a]	228	0.22 ± 0.10	1.92 ± 0.07	2.48 ± 0.09
34[a]	433	0.21 ± 0.05	1.91 ± 0.04	2.46 ± 0.05
213[a]	357	0.58 ± 0.08	4.25 ± 0.30	5.48 ± 0.40
214[a]	294	0.57 ± 0.08	4.24 ± 0.30	5.47 ± 0.35

[a]The micelle structures used for COSMOmic calculations were taken from a 200 ns MD simulation of 0.22 mol/L Triton X-100 solution.

Table 8. Predicted Partition Coefficients of 6 Neutral Solutes in Triton X-100 Micelles in Comparison with Experimental Data[82,83]

	$\log P^{MW,COSMOmic}$				
solute	N_{agg} = 33[a]	N_{agg} = 34[a]	N_{agg} = 213[a]	N_{agg} = 214[a]	$\log P^{MW,exp}$
pyrene[b]	4.31	4.33	3.31	3.33	4.49
phenanthrene[b]	4.01	4.03	3.07	3.09	4.16
naphthalene[b]	3.18	3.21	2.37	2.38	3.10
phenol[c]	1.95	1.98	1.58	1.59	1.79
vanillin[c]	2.00	2.01	1.58	1.59	1.90
3-methoxyphenol[c]	2.10	2.13	1.73	1.74	1.96
RMSE	0.14	0.15	0.74	0.73	

[a]The micelle structures used for COSMOmic calculations were taken from a 200 ns MD simulation of 0.22 Triton X-100 solution. [b]The partition coefficients are measured and calculated at 298 K.[83] [c]The partition coefficients are measured and calculated at 293 K.[82]

agreement with experimental data (RMSE = 0.14 and 0.15, respectively). The usage of small Triton X-100 micelles (aggregation number ~33) shows better prediction quality (RMSE ~0.15) compared to the calculations using Triton X-114 micelles of the same size (RMSE ~0.40). Since no significant difference in the micelle structures is observed (aggregation number, micelle radius, and eccentricity factor are in the same range), it can be concluded that the deviation is due to the different solutes which were studied. The predicted partition coefficients using larger micelles (N_{agg} = 213 and N_{agg} = 214) underestimate the experimentally determined partition coefficients with RMSE = 0.74 and RMSE = 0.73, respectively. Consequently, when using large micelles (R_s > 5 nm) outliers can occur. The reason is the deviation of the structure from a sphere (see ε in Table 7). This could lead to decline of the prediction quality; as in COSMOmic the micelle structure is assumed as a perfect sphere surrounded by a water shell.

Hence, the main factor that influences the quality of the COSMOmic predictions is the form of the micelle, defined by the eccentricity factor.[40] In a previous study[40] it has been recommended to use spherical micelles ($\varepsilon \leq 0.5$), since the prediction quality decreases for cylindrical micelles. These findings are in line with the results presented in this work. Therefore, in order to achieve appropriate prediction quality with COSMOmic, the micelles formed during the MD simulations need to be analyzed and selected according to their structure. Although cylindrical micelles ($\varepsilon \geq 0.5$) can also provide good prediction quality (see Table 6), outliers are more likely to occur. On the other hand, when using small spherical micelles (R_s < 4 nm, $\varepsilon \leq 0.5$) as input structures for the COSMOmic calculation, all predicted partition coefficients are in very good agreement with experimental data (RMSE ≤ 0.42). Therefore, we recommend to select micelle structures from MD according to their structural parameters (radius of the micelle and eccentricity factor) and by checking the radial densities: small spherical micelles without gaps in the water shell.

4. CONCLUSIONS

In this work, the self-assembly of the surfactants Triton X-114 and Triton X-100 in aqueous solution at different concentrations and temperatures was studied via all-atom MD simulations. Since the Triton X molecules are not present in any known biomolecular force field, we have developed the first optimized set of Triton X-114 parameters for the CHARMM general force field. Optimized force field parameters have been obtained using the ffTK. The parameter validation is challenging, as there is insufficient experimental data for Triton X-114. In addition to micelle structure and partition coefficient analysis a bulk phase simulation was carried out to validate the ability of the force field parameters to reproduce the experimental pure solvent density. The calculated density of Triton X-114 is in excellent agreement with experimental results. The obtained force field parameters can be used to model other molecules from the Triton X-series, as they differ only by their poly(ethylene oxide) chain length.

DOI: 10.1021/acs.jctc.5b00026
J. Chem. Theory Comput. XXXX, XXX, XXX−XXX

In the MD simulations micelles of different size are formed, which is characteristic for the polydisperse solutions of nonionic surfactants.[75−77] The results are discussed considering the size (aggregation number), shape, and structure of micellar aggregates as a function of temperature and surfactant concentration. The aggregation number increases with increasing temperature and surfactant concentration, which is in agreement with experimental data.[80]

Furthermore, the micelle structures obtained from the MD simulations were used as input for the model COSMOmic in order to predict the partition behavior of small neutral solutes (mostly acids), whereby the influence of the micellar structures on the partition behavior was studied. More chemically diverse molecules could not be considered in this work due to the lack of available experimental data. In general, the predicted partition coefficients are in very good agreement with experimental data. In order to achieve statistical reliable results, we used averaged atomic distributions for the micelle structure. This approach reduces the effect of outliers. It is important to note that COSMOmic assumes the micelle structure to be a sphere. Therefore, by comparing the predictions of the partition coefficients using different micelle structures, an influence of the micelle size and shape on the prediction quality was observed. When using large or more cylindrical micelles, outliers are more likely to occur. Thus, we can recommend a selection of the micelle structures by their size and form (small and spherical). Whereas the micelle structure is problematic for large micelles, for small micelles the water layer around the micelle can be problematic.[41] COSMOmic assumes the last layer to be the second phase (i.e., the water phase). However, in self-assembly simulations other micelles or surfactant molecules are present such that sometimes no bulk water is found around the micelle. This problem was solved in this work by replacing the disturbing molecules by water in the distributions used for COSMOmic. We can conclude that the combination of micelles obtained from MD simulations with COSMOmic successfully predict partition behavior of neutral solutes. Advantageous, once a micelle structure is obtained, it is possible to calculate partition coefficients of multiple solutes in only a few minutes, which make it suitable as a screening tool for solute partition behavior.

In summary, this article introduces force field parameters for Triton X-series which leads to reasonable simulation results compared to available experimental data. Furthermore, it was shown that the combinations of MD simulation and COSMOmic result in good partition coefficient predictions.

■ ASSOCIATED CONTENT

Ⓢ Supporting Information

Additional tables, which include the optimized parameters for the Triton X molecules (partial charges, bonds, angles, dihedrals). This material is available free of charge via the Internet at http://pubs.acs.org.

■ AUTHOR INFORMATION

Corresponding Author

*E-mail: jakobtorweihen@tuhh.de.

Notes

The authors declare no competing financial interest.

■ ACKNOWLEDGMENTS

The authors appreciate financial support of the German Academic Exchange Service (DAAD) and from the Hamburg University of Technology research center "Integrated Biotechnology and Process Engineering". Computational resources have been provided by The North-German Supercomputing Alliance (HLRN).

■ REFERENCES

(1) Sanguansri, P.; Augustin, M. A. Nanoscale materials development - a food industry perspective. *Trends Food Sci. Technol.* **2006**, *17*, 547−556.

(2) Esmaili, M.; Ghaffari, S. M.; Moosavi-Movahedi, Z.; Atri, M. S.; Sharifizadeh, A.; Farhadi, M.; Yousefi, R.; Chobert, J.-M.; Haertlé, T.; Moosavi-Movahedi, A. A. Beta casein-micelle as a nano vehicle for solubility enhancement of curcumin; food industry application. *LWT - Food Sci. Technol.* **2011**, *44*, 2166−2172.

(3) Kataoka, K.; Harada, A.; Nagasaki, Y. Block copolymer micelles for drug delivery: design, characterization and biological significance. *Adv. Drug Delivery Rev.* **2001**, *47*, 113−131.

(4) Nasongkla, N.; Bey, E.; Ren, J.; Ai, H.; Khemtong, C.; Guthi, J. S.; Chin, S.-F.; Sherry, A. D.; Boothman, D. A.; Gao, J. Multifunctional Polymeric Micelles as Cancer-Targeted, MRI-Ultrasensitive Drug Delivery Systems. *Nano Lett.* **2006**, *6*, 2427−2430.

(5) Nishi, H. Pharmaceutical applications of micelles in chromatography and electrophoresis. *J. Chromatogr. A* **1997**, *780*, 243−264.

(6) Helenius, A.; Simons, K. Solubilization of membranes by detergents. *Biochim. Biophys. Acta* **1975**, *415*, 29−79.

(7) Tanford, C.; Reynolds, J. A. Characterization of membrane proteins in detergent solutions. *Biochim. Biophys. Acta* **1976**, *457*, 133−170.

(8) Wennerström, H. Micelles. Physical chemistry of surfactant association. *Phys. Rep.* **1979**, *52*, 1−86.

(9) Lichtenberg, D.; Robson, R. J.; Dennis, E. A. Solubilization of phospholipids by detergents structural and kinetic aspects. *Biochim. Biophys. Acta* **1983**, *737*, 285−304.

(10) le Maire, M.; Champeil, P.; Møller, J. V. Interaction of membrane proteins and lipids with solubilizing detergents. *Biochim. Biophys. Acta* **2000**, *1508*, 86−111.

(11) Dickie, P.; Weiner, J. H. Purification and characterization of membrane-bound fumarate reductase from anaerobically grown *Escherichia coli*. *Can. J. Biochem.* **1979**, *57*, 813−821.

(12) Nicholson, D.; McMurray, W. Triton solubilization of proteins from pig liver mitochondrial membranes. *Biochim. Biophys. Acta* **1986**, *856*, 515−525.

(13) Egan, W. R. Hydrophile-lipophile balance and critical micelle concentration as key factors influencing surfactant disruption of mitochondrial membranes. *J. Biol. Chem.* **1976**, *251*, 4442−4447.

(14) Umbreit, J. N.; Strominger, J. L. Relation of Detergent HLB Number to Solubilization and Stabilization of D-Alanine Carboxypeptidase from Bacillus subtilis Membranes. *Proc. Natl. Acad. Sci. U.S.A.* **1973**, *70*, 2997−3001.

(15) Bordier, C. Phase separation of integral membrane proteins in Triton X-114 solution. *J. Biol. Chem.* **1981**, *256*, 1604−1607.

(16) Florke, R.-R.; Klein, H. W.; Reinauer, H. Differential insertion of insulin receptor complexes into Triton X-114 bilayer membranes. Evidence for a differential accessibility of the membrane-exposed receptor domain. *Eur. J. Biochem.* **1993**, *211*, 241−247.

(17) Sivars, U.; Tjerneld, F. Mechanisms of phase behaviour and protein partitioning in detergent/polymer aqueous two-phase systems for purification of integral membrane proteins. *Biochim. Biophys. Acta* **2000**, *1474*, 133−146.

(18) Brusca, J. S., Radolf, J. D. *Methods in Enzymology*; Elsevier: 1994; Vol. *228*; pp 182−193.

(19) Mathias, R. A.; Chen, Y.-S.; Kapp, E. A.; Greening, D. W.; Mathivanan, S.; Simpson, R. J. Triton X-114 phase separation in the isolation and purification of mouse liver microsomal membrane proteins. *Methods* **2011**, *54*, 396−406.

DOI: 10.1021/acs.jctc.5b00026
J. Chem. Theory Comput. XXXX, XXX, XXX−XXX

(20) Chen, J.; Teo, K. C. Determination of cobalt and nickel in water samples by flame atomic absorption spectrometry after cloud point extraction. *Anal. Chim. Acta* **2001**, *434*, 325−330.
(21) Tang, A. N.; Jiang, D. Q.; Yan, X. P. Cloud point extraction preconcentration for capillary electrophoresis of metal ions. *Anal. Chim. Acta* **2004**, *507*, 199−204.
(22) Niazi, A.; Momeni-Isfahani, T.; Ahmari, Z. Spectrophotometric determination of mercury in water samples after cloud point extraction using nonionic surfactant Triton X-114. *J. Hazard. Mater.* **2009**, *165*, 1200−1203.
(23) Ingram, T.; Storm, S.; Glembin, P.; Bendt, S.; Huber, D.; Mehling, T.; Smirnova, I. Aqueous Surfactant Two-Phase Systems for the Continuous Countercurrent Cloud Point Extraction. *Chem. Ing. Tech.* **2012**, *84*, 840−848.
(24) Glembin, P.; Racheva, R.; Kerner, M.; Smirnova, I. Micelle mediated extraction of fatty acids from microalgae cultures: Implementation for outdoor cultivation. *Sep. Purif. Technol.* **2014**, *135*, 127−134.
(25) Arunagiri, A.; Priya, K.; Kalaichelvi, P.; Anantharaj, R. Extraction of Reactive Orange 107 dye from aqueous stream using Triton X-114 surfactant: Quantum chemical calculations and experiment. *J. Ind. Eng. Chem.* **2014**, *20*, 2409−2420.
(26) Xing, W.; Chen, L.; Zhang, F. Separation of camptothecin from Camptotheca acuminate samples using cloud point extraction. *Anal. Methods* **2014**, *6*, 3644.
(27) Xia, Q.; Jiao, Y.; Xiong, W.; Yang, Y.; Liu, M. Development of a Precolumn Derivatization Procedure Prior to Ultrasound-Assisted Cloud Point Extraction for Sensitive Determination of Fluoroquinolones in Eggs by High-Performance Liquid Chromatography with Fluorescence Detection. *Food Anal. Methods* **2014**, *7*, 1130−1138.
(28) Buggert, M.; Cadena, C.; Mokrushina, L.; Smirnova, I.; Maginn, E. J.; Arlt, W. COSMO-RS Calculations of Partition Coefficients: Different Tools for Conformation Search. *Chem. Eng. J.* **2009**, *32*, 977−986.
(29) Pastor, R. W.; MacKerell, A. D. Development of the CHARMM Force Field for Lipids. *J. Phys. Chem. Lett.* **2011**, *2*, 1526−1532.
(30) Klauda, J. B.; Venable, R. M.; Freites, J. A.; O'Connor, J. W.; Tobias, D. J.; Mondragon-Ramirez, C.; Vorobyov, I.; MacKerell, A. D.; Pastor, R. W. Update of the CHARMM All-Atom Additive Force Field for Lipids: Validation on Six Lipid Types. *J. Phys. Chem. B* **2010**, *114*, 7830−7843.
(31) Vanommeslaeghe, K.; Hatcher, E.; Acharya, C.; Kundu, S.; Zhong, S.; Shim, J.; Darian, E.; Guvench, O.; Lopes, P.; Vorobyov, I.; Mackerell, A. D. CHARMM general force field: A force field for drug-like molecules compatible with the CHARMM all-atom additive biological force fields. *J. Comput. Chem.* **2009**, *31*, 671−690.
(32) Cheng, X.; Jo, S.; Lee, H. S.; Klauda, J. B.; Im, W. CHARMM-GUI Micelle Builder for Pure/Mixed Micelle and Protein/Micelle Complex Systems. *J. Chem. Inf. Model.* **2013**, *53*, 2171−2180.
(33) Klamt, A.; Huniar, U.; Spycher, S.; Keldenich, J. COSMOmic: A Mechanistic Approach to the Calculation of Membrane-Water Partition Coefficients and Internal Distributions within Membranes and Micelles. *J. Phys. Chem. B* **2008**, *112*, 12148−12157.
(34) Klamt, A. Conductor-like Screening Model for Real Solvents: A New Approach to the Quantitative Calculation of Solvation Phenomena. *J. Phys. Chem.* **1995**, *99*, 2224−2235.
(35) Klamt, A.; Jonas, V.; Bürger, T.; Lohrenz, J. C. W. Refinement and Parametrization of COSMO-RS. *J. Phys. Chem. A* **1998**, *102*, 5074−5085.
(36) Klamt, A.; Eckert, F. COSMO-RS: a novel and efficient method for the a priori prediction of thermophysical data of liquids. *Fluid Phase Equilib.* **2000**, *172*, 43−72.
(37) Klamt, A.; Eckert, F.; Arlt, W. COSMO-RS: An Alternative to Simulation for Calculating Thermodynamic Properties of Liquid Mixtures. *Annu. Rev. Chem. Biomol. Eng.* **2010**, *1*, 101−122.
(38) Klamt, A. The COSMO and COSMO-RS solvation models. *Wiley Interdiscip. Rev.: Comput. Mol. Sci.* **2011**, *1*, 699−709.
(39) Ingram, T.; Storm, S.; Kloss, L.; Mehling, T.; Jakobtorweihen, S.; Smirnova, I. Prediction of Micelle/Water and Liposome/Water Partition Coefficients Based on Molecular Dynamics Simulations, COSMO-RS, and COSMOmic. *Langmuir* **2013**, *29*, 3527−3537.
(40) Storm, S.; Jakobtorweihen, S.; Smirnova, I.; Panagiotopoulos, A. Z. Molecular Dynamics Simulation of SDS and CTAB Micellization and Prediction of Partition Equilibria with COSMOmic. *Langmuir* **2013**, *29*, 11582−11592.
(41) Storm, S.; Jakobtorweihen, S.; Smirnova, I. Solubilization in Mixed Micelles Studied by Molecular Dynamics Simulations and COSMOmic. *J. Phys. Chem. B* **2014**, *118*, 3593−3604.
(42) Endo, S.; Escher, B. I.; Goss, K.-U. Capacities of Membrane Lipids to Accumulate Neutral Organic Chemicals. *Environ. Sci. Technol.* **2011**, *45*, 5912−5921.
(43) Jakobtorweihen, S.; Ingram, T.; Smirnova, I. Combination of COSMOmic and molecular dynamics simulations for the calculation of membrane-water partition coefficients. *J. Comput. Chem.* **2013**, *34*, 1332−1340.
(44) Jakobtorweihen, S.; Zuniga, A. C.; Ingram, T.; Gerlach, T.; Keil, F. J.; Smirnova, I. Predicting solute partitioning in lipid bilayers: Free energies and partition coefficients from molecular dynamics simulations and COSMOmic. *J. Chem. Phys.* **2014**, *141*, 045102.
(45) Paloncýová, M.; DeVane, R.; Murch, B.; Berka, K.; Otyepka, M. Amphiphilic Drug-Like Molecules Accumulate in a Membrane below the Head Group Region. *J. Phys. Chem. B* **2014**, *118*, 1030−1039.
(46) Geiger, H. C.; Lamson, M.; Galka, D. J. Synthesis and Spectroscopic Characterization of Chiral Biphenyl-Cholesterol Gels. *Langmuir* **2014**, *30*, 13979−13986.
(47) Mayne, C. G.; Saam, J.; Schulten, K.; Tajkhorshid, E.; Gumbart, J. C. Rapid parameterization of small molecules using the force field toolkit. *J. Comput. Chem.* **2013**, *34*, 2757−2770.
(48) Humphrey, W.; Dalke, A.; Schulten, K. VMD - Visual Molecular Dynamics. *J. Mol. Graphics* **1996**, *14*, 33−38.
(49) Frisch, M. J., Trucks, G. W., Schlegel, H. B., Scuseria, G. E., Robb, M. A., Cheeseman, J. R., Montgomery, J. A., Jr., Vreven, T., Kudin, K. N., Burant, J. C., Millam, J. M., Iyengar, S. S., Tomasi, J., Barone, V., Mennucci, B., Cossi, M., Scalmani, G., Rega, N., Petersson, G. A., Nakatsuji, H., Hada, M., Ehara, M., Toyota, K., Fukuda, R., Hasegawa, J., Ishida, M., Nakajima, T., Honda, Y., Kitao, O., Nakai, H., Klene, M., Li, X., Knox, J. E., Hratchian, H. P., Cross, J. B., Bakken, V., Adamo, C., Jaramillo, J., Gomperts, R., Stratmann, R. E., Yazyev, O., Austin, A. J., Cammi, R., Pomelli, C., Ochterski, J. W., Ayala, P. Y., Morokuma, K., Voth, G. A., Salvador, P., Dannenberg, J. J., Zakrzewski, V. G., Dapprich, S., Daniels, A. D., Strain, M. C., Farkas, O., Malick, D. K., Rabuck, A. D., Raghavachari, K., Foresman, J. B., Ortiz, J. V., Cui, Q., Baboul, A. G., Clifford, S., Cioslowski, J., Stefanov, B. B., Liu, G., Liashenko, A., Piskorz, P., Komaromi, I., Martin, R. L., Fox, D. J., Keith, T., Al-Laham, M. A., Peng, C. Y., Nanayakkara, A., Challacombe, M., Gill, P. M. W., Johnson, B., Chen, W., Wong, M. W., Gonzalez, C., Pople, J. A. *Gaussian 03, Revision C.02*; Gaussian, Inc.: Wallingford, CT, 2004.
(50) Vanommeslaeghe, K.; MacKerell, A. D. Automation of the CHARMM General Force Field (CGenFF) I: Bond Perception and Atom Typing. *J. Chem. Inf. Model.* **2012**, *52*, 3144−3154.
(51) Vanommeslaeghe, K.; Raman, E. P.; MacKerell, A. D. Automation of the CHARMM General Force Field (CGenFF) II: Assignment of Bonded Parameters and Partial Atomic Charges. *J. Chem. Inf. Model.* **2012**, *52*, 3155−3168.
(52) Jorgensen, W. L.; Chandrasekhar, J.; Madura, J. D.; Impey, R. W.; Klein, M. L. Comparison of simple potential functions for simulating liquid water. *J. Chem. Phys.* **1983**, *79*, 926.
(53) Pronk, S.; Pall, S.; Schulz, R.; Larsson, P.; Bjelkmar, P.; Apostolov, R.; Shirts, M. R.; Smith, J. C.; Kasson, P. M.; van der Spoel, D.; Hess, B.; Lindahl, E. GROMACS 4.5: a high-throughput and highly parallel open source molecular simulation toolkit. *Bioinformatics* **2013**, *29*, 845−854.
(54) Tang, X.; Koenig, P. H.; Larson, R. G. Molecular Dynamics Simulations of Sodium Dodecyl Sulfate Micelles in Water-The Effect of the Force Field. *J. Phys. Chem. B* **2014**, *118*, 3864−3880.
(55) MacKerell, A. D.; Bashford, D.; Bellott, M.; Dunbrack, R. L.; Evanseck, J. D.; Field, M. J.; Fischer, S.; Gao, J.; Guo, H.; Ha, S.;

DOI: 10.1021/acs.jctc.5b00026
J. Chem. Theory Comput. XXXX, XXX, XXX−XXX

Joseph-McCarthy, D.; Kuchnir, L.; Kuczera, K.; Lau, F. T. K.; Mattos, C.; Michnick, S.; Ngo, T.; Nguyen, D. T.; Prodhom, B.; Reiher, W. E.; Roux, B.; Schlenkrich, M.; Smith, J. C.; Stote, R.; Straub, J.; Watanabe, M.; Wiórkiewicz-Kuczera, J.; Yin, D.; Karplus, M. All-Atom Empirical Potential for Molecular Modeling and Dynamics Studies of Proteins. *J. Phys. Chem. B* **1998**, *102*, 3586−3616.

(56) Durell, S. R.; Brooks, B. R.; Ben-Naim, A. Solvent-Induced Forces between Two Hydrophilic Groups. *J. Phys. Chem.* **1994**, *98*, 2198−2202.

(57) Darden, T.; York, D.; Pedersen, L. Particle mesh Ewald: An N.log(N) method for Ewald sums in large systems. *J. Chem. Phys.* **1993**, *98*, 10089.

(58) Essmann, U.; Perera, L.; Berkowitz, M. L.; Darden, T.; Lee, H.; Pedersen, L. G. A smooth particle mesh Ewald method. *J. Chem. Phys.* **1995**, *103*, 8577.

(59) Hess, B. P-LINCS: A Parallel Linear Constraint Solver for Molecular Simulation. *J. Chem. Theory Comput.* **2008**, *4*, 116−122.

(60) Sammalkorpi, M.; Karttunen, M.; Haataja, M. Structural Properties of Ionic Detergent Aggregates: A Large-Scale Molecular Dynamics Study of Sodium Dodecyl Sulfate. *J. Phys. Chem. B* **2007**, *111*, 11722−11733.

(61) MacKerell, A. D. Molecular Dynamics Simulation Analysis of a Sodium Dodecyl Sulfate Micelle in Aqueous Solution: Decreased Fluidity of the Micelle Hydrocarbon Interior. *J. Phys. Chem.* **1995**, *99*, 1846−1855.

(62) Salaniwal, S.; Cui, S. T.; Cochran, H. D.; Cummings, P. T. Molecular Simulation of a Dichain Surfactant/Water/Carbon Dioxide System. 1. Structural Properties of Aggregates. *Langmuir* **2001**, *17*, 1773−1783.

(63) Klamt, A.; Eckert, F.; Diedenhofen, M. Prediction or partition coefficients and activity coefficients of two branched compounds using COSMOtherm. *Fluid Phase Equilib.* **2009**, *285*, 15−18.

(64) Mokrushina, L.; Yamin, P.; Sponsel, E.; Arlt, W. Prediction of phase equilibria in systems containing large flexible molecules using COSMO-RS: State-of-the-problem. *Fluid Phase Equilib.* **2012**, *334*, 37−42.

(65) Ahlrichs, R.; Bär, M.; Häser, M.; Horn, H.; Kölmel, C. Electronic structure calculations on workstation computers: The program system turbomole. *Chem. Phys. Lett.* **1989**, *162*, 165−169.

(66) Perdew, J. Density-functional approximation for the correlation energy of the inhomogeneous electron gas. *Phys. Rev. B: Condens. Matter Mater. Phys.* **1986**, *33*, 8822−8824.

(67) Becke, A. D. Density-functional exchange-energy approximation with correct asymptotic behavior. *Phys. Rev. A: At., Mol., Opt. Phys.* **1988**, *38*, 3098−3100.

(68) Schäfer, A.; Huber, C.; Ahlrichs, R. Fully optimized contracted Gaussian basis sets of triple zeta valence quality for atoms Li to Kr. *J. Chem. Phys.* **1994**, *100*, 5829.

(69) Eichkorn, K.; Treutler, O.; Öhm, H.; Häser, M.; Ahlrichs, R. Auxiliary basis sets to approximate Coulomb potentials. *Chem. Phys. Lett.* **1995**, *242*, 652−660.

(70) HyperChem. HyperChem Profesional Overview. http://www.hyper.com/?TabId=361 (accessed May 29, 2013).

(71) Hegazy, L.; Richards, N. G. J. Optimized CGenFF force-field parameters for acylphosphate and N-phosphonosulfonimidoyl functional groups. *J. Mol. Model.* **2013**, *19*, 5075−5087.

(72) Linke, D. *Methods in Enzymology*; Elsevier: 2009; Vol. *463*; pp 603−617.

(73) Panayotova, S.; Bivas, I. Borders of the Liquid Crystalline Phase in the Triton X-114 - Water Binary System. *Bulg. J. Phys.* **2004**, *31*, 83−86.

(74) Tani, H.; Kamidate, T.; Watanabe, H. Aqueous Micellar Two-Phase Systems for Protein Separation. *Anal. Sci.* **1998**, *14*, 875−888.

(75) Brown, W.; Pu, Z.; Rymden, R. Size and shape of nonionic amphiphile micelles: NMR self-diffusion and static and quasi-elastic light-scattering measurements on C12E5, C12E7, and C12E8 in aqueous solution. *J. Phys. Chem.* **1988**, *92*, 6086−6094.

(76) Magid, L. J.; Triolo, R.; Johnson, J. S. Small-angle neutron-scattering study of critical phenomena in aqueous solutions of C12E8, an nonionic amphiphile. *J. Phys. Chem.* **1984**, *88*, 5730−5734.

(77) Brown, W.; Rymden, R.; van Stam, J.; Almgren, M.; Svensk, G. Static and dynamic properties of nonionic amphiphile micelles: Triton X-100 in aqueous solution. *J. Phys. Chem.* **1989**, *93*, 2512−2519.

(78) Wolszczak, M.; Miller, J. Characterization of non-ionic surfactant aggregates by fluorometric techniques. *J. Photochem. Photobiol., A* **2002**, *147*, 45−54.

(79) Ingram, T.; Mehling, T.; Smirnova, I. Partition coefficients of ionizable solutes in aqueous micellar two-phase systems. *Chem. Eng. J.* **2013**, *218*, 204−213.

(80) McCarroll, M. E.; Toerne, K.; von Wandruszka, R. Preclouding in Mixed Micellar Solutions. *Langmuir* **1998**, *14*, 6096−6100.

(81) Patel, V.; Ray, D.; Aswal, V. K.; Bahadur, P. Triton X-100 micelles modulated by solubilized cinnamic acid analogues: The pH dependant micellar growth. *Colloids Surf., A* **2014**, *450*, 106−114.

(82) Mehling, T.; Ingram, T.; Smirnova, I. Experimental Methods and Prediction with COSMO-RS to Determine Partition Coefficients in Complex Surfactant Systems. *Langmuir* **2012**, *28*, 118−124.

(83) Edwards, D. A.; Luthy, R. G.; Liu, Z. Solubilization of polycyclic aromatic hydrocarbons in micellar nonionic surfactant solutions. *Environ. Sci. Technol.* **1991**, *25*, 127−133.

DOI: 10.1021/acs.jctc.5b00026
J. Chem. Theory Comput. XXXX, XXX, XXX−XXX